SPE 143589

Experimental and Simulation Analysis of CO_2 Storage in Tight and Fractured Sandstone under Different Stress Conditions

R. Farokhpoor, T.Baghbanbashi, O.Torsæter, NTNU, E. Lindeberg, SINTEF, A. Mørk, NTNU, SINTEF

Abstract

Sequestration of carbon dioxide in a saline aquifer into shallow marine formation of Jurassic sandstones in Svalbard has been studied on unfractured cores and by using a simplified set of geological boundary conditions. In this paper, the feasibility of storing CO_2 in a fracture and matrix system in a low permeable formation is studied by performing a series of laboratory experiments under different stress conditions. Laboratory core flooding experiments were conducted on two alternative fractured and unfractured cores. Water and nitrogen were injected into brine saturated cores at the reservoir conditions. The result shows that core plugs are very tight and the liquid permeability even for fractured core is less than 1 millidarcy. Under increased acting stress from 10 to 180 bar, the effective permeability of fractured core is reduced by 73 percent and fluid flow occurs through both fracture and matrix.

A conceptual, generic and simple 3D numerical model using commercial reservoir simulation software and available petrophysical data was used to study the CO_2 injection through fracture at different overburden pressure. The effect of different overburden pressures were applied by using respective permeabilities in simulation model. Mean pressure along the cores was used to match simulation predictions with experiments results. The result shows that even though the system is water-wet, and matrix has a very high capillary pressure, CO_2 flows through both fracture and matrix. The amount of CO_2 that flows through the fracture is high and is reduced by increasing overburden pressure. The quantity of dissolved CO_2 in brine phase reduces by decreasing overburden pressure and increasing permeability. The faster the CO_2 is flowing through the fracture less time is available for CO_2 to trap as residual phase and dissolve in brine. In dipping fractured saline aquifer, CO_2 plume movement in updip direction is accelerated by decreased overburden pressure and increased permeability.

Introduction

The first and foremost task for carbon capture and storage is to find suitable locations to permanently sequester CO_2 which are injected into the reservoir. A research project is investigating the possibility of storing CO_2 from the local power plant station in the subsurface at 670-1000 m depth (Olaussen, et al., 2011). Most of the reservoirs contain fractures to some extent. Based on research from various scientific studies, reservoirs with fractures may cause leakage problems which will be detrimental to the environment and safety (Huo & Gong, 2010). Natural fractures in cap rock could potentially allow CO_2 to quickly migrate through the cap rock to the surface. In low permeable saline aquifer, since fracture is preferential flow path, it enhances CO_2 storage and injectivity. In dipping fractured aquifer, CO_2 encounters permeability increase subjected to the reduced overburden pressure in upward direction. These fractures are regarded as potential escape routes for CO_2, which could threat prospective storage ability of a specific storage site.

In previous study from same authors, a conceptual study of reservoir behaviour of CO_2 storage into shallow marine

formation of Upper-Triassic to Mid-Jurassic sandstones in Svalbard has been done on unfractured cores. The reservoir sandstones have been described before (Farokhpoor *et al.*, 2010). The studied samples are from the Longyearbyen CO_2 Lab, and the results showed very low permeability in unfractured samples, 0.01 to 2.0 mD. This is typically too low permeability to allow effective injection and storage of CO_2. Short injection tests in the intended storage site showed that the formation has fairly good injectivity suggesting the presence of fractures. The new sampling in heterogeneous zones reveals that there are fractures galore in the core and fractures all over the outcrop lining up with a regional stress pattern. The fractures in the core even show mm sized apertures at standard condition in the surface cementation (Senger *et al.*, 2011).

In this study, the permeability variations in fractured and unfractured cores at different overburden pressures were investigated. A conceptual, generic and simple 3D aquifer model in laboratory scale is used to study the fluid flow through the fracture at different overburden pressures. The laboratory process, in which the water was injected through the fracture, is duplicated in this modeling effort. Later on, a physical CO_2 injection process is applied to the validated model to study the CO_2 flow through the fractures.

Experimental works

All the experiments were conducted on two pebbly sandstone samples plugged in the same rock formation and in neighboring locations. These samples are taken from the depth 676.9-677.1 m which is formed by poorly sorted sand with scattered gravel. The upper one is fractured while the lower sample is homogeneous and represents matrix properties. The petrophysical properties of both cores are summarized in **Table 1**.

Table 1: Samples properties

Property	*Unfractured sample*	*Fractured sample*
Depth, m	677.0	676.9
Length, cm	4.86	9.62
Diameter, cm	3.77	4.75
Water Porosity	15 %	10 %

The studied samples (**Figure 1**) represent polymictic conglomerate with sandstone matrix. The samples are a remanie conglomerate with pebbles of quartz, chert, quartzite, claystone and phosphate within a matrix of sandstone. The sandstones low permeability is due to irregular microstructure of quartz cemented tight domenes alternating with clay rich domains (Mørk & Farokhpoor, 2011). A X-ray CT scanner was used to envisage fracture profile and its extension along a fractured core, which is shown in Figure 1**.** The light color shows the particles with higher density.

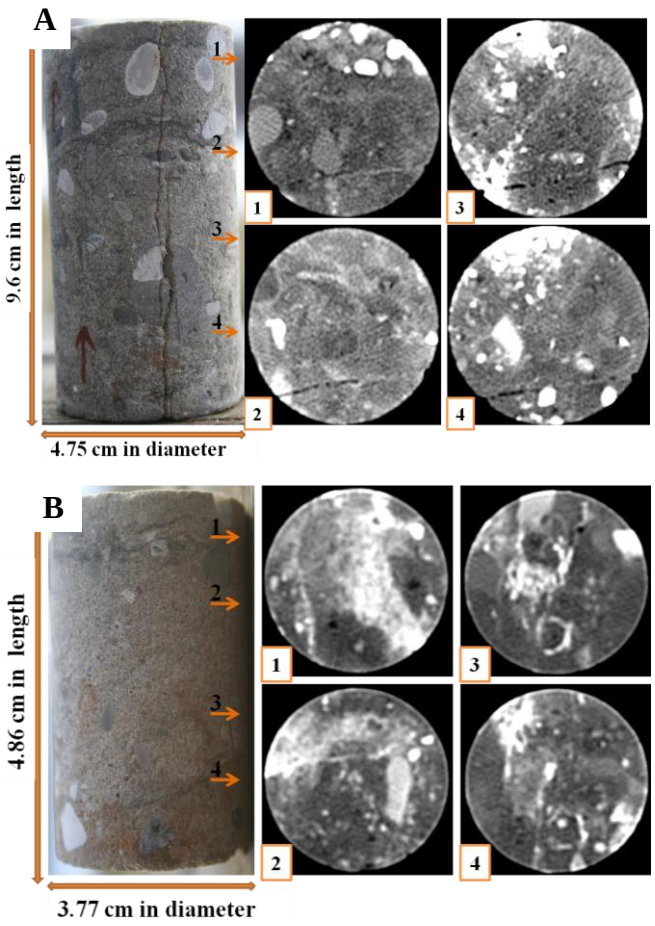

Figure 1: The CT studied sandstone samples. Note the polymictic nature of the conglomerate within a bioturbated sandstone matrix. The circles to the right are CT scans at the indicated depth. The core is 47 mm in diameter and the fracture that is nearly vertical in the picture show dark porosity interrupted by thin lighter areas. These may represent calcite cement as weak bubbling is observed with HCl. b) The lower sample, 37 mm in diameter, do not show any fractures, but color variation due to the polymictic conglomerate.

In this study, fluid flow experiments were performed on both homogeneous and fractured cores with different overburden pressures and injection rates. The experimental set-up is designed to work under representative reservoir conditions up to 200 bar and 22°C. Its main components are a Hassler-type core holder and a pumping system that allows brine and nitrogen injections. The brine used in the experiment

contains 36 g NaCl mixed by one liter distilled water which results in the brine density of 1.04 g/cm^3. The clean core was inserted the Hassler core holder using 100 bar confining pressure. Core flooding was performed with different injection rates. After running a set of injection rates under this pressure, the confining pressure was changed and the injection was continued with different rates. Similar procedure was performed using unfractured core. The experimental set up is shown in **Figure 2**.

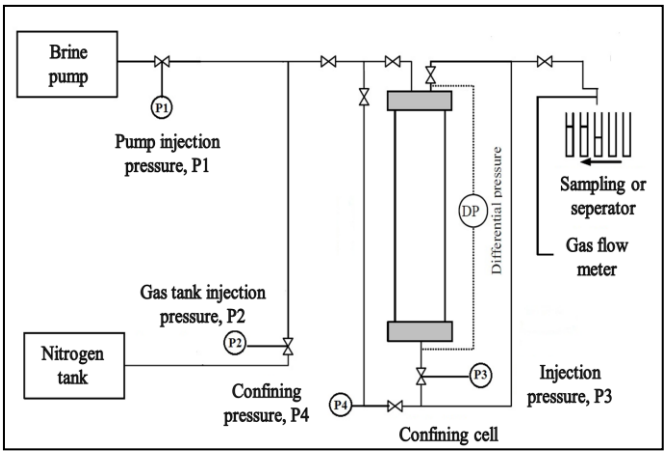

Figure 2: A schematic of experimental set-up

All the experiments were repeated with nitrogen. The brine is injected directly with a high pressure pump, while the nitrogen was delivered directly from a high pressure bottle. First the core flooding is conducted with brine and later the cores are removed and cleaned by methanol and prepared for measuring absolute permeability by nitrogen.

Three different confining pressures (100, 140 and 180 bar) were applied for both unfractured and fractured cores. The confining pressure is ensured by a Viton sleeve with 5 mm thickness. At the brine injection process, the injection rates ranged from 0.1 to 0.6 ml/min and were performed at each overburden pressure. After each change in injection rate, the system is left to reach to the steady state and then the pressure at the injection point is recorded. The injection pressure is controlled by injection rate and confining pressure. The outlet is opened to atmospheric pressure and a sampling device is connected to collect fluid downstream. In the case of nitrogen injection, the gas line is equipped with a gas flow meter to measure the gas flow rate. Since the lab temperature (22°C) is so close to the actual reservoir temperature (28°C), the experiments were performed without other temperature control. **Table 2** lists the operating conditions of the experiments, recorded effective overburden pressure and measured permeability. The effective overburden pressure is the difference of applied confining pressure and mean pressure along the core plug. **Figure 3** shows the comparison of permeability reduction between unfractured and fractured core at increased overburden pressure.

Table 2: Experimental observations for fractured and unfractured core

Overburden pressure bar	*Flow rate ml/min*	*Permeability of fractured core, mD*	*Permeability of unfractured core, mD*
80.0	0.6	0.118	0.0653
83.5	0.5	0.115	0.0638
86.7	0.4	0.109	0.0611
118.0	0.4	0.086	0.0609
122.5	0.3	0.081	0.0594
127.5	0.2	0.075	0.0583
159.0	0.4	0.063	0.0573
156.0	0.3	0.059	0.0556
163.5	0.2	0.057	0.0548
171.5	0.1	0.055	0.0539

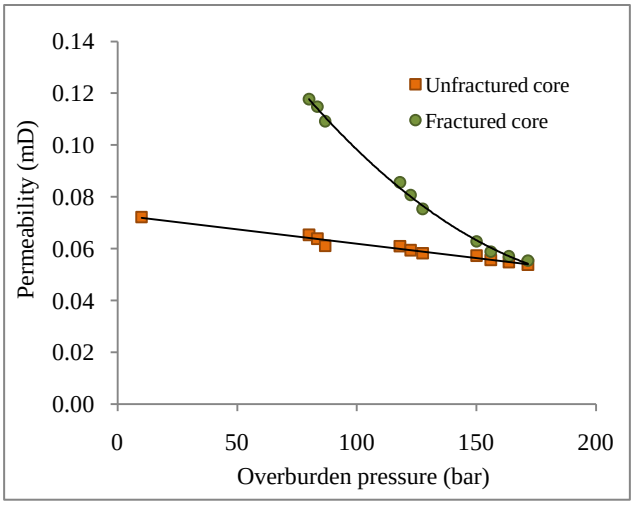

Figure 3: Permeability variations for fractured and unfractured core versus overburden pressure

In fractured core, as the effective overburden pressure increases from 10 to 180 bar, liquid permeability decreases by 73 percent. Meanwhile, the liquid permeability in unfractured core is reduced just by 24 percent at the same overburden pressure range. The same procedure is applied by injecting nitrogen into the fractured core. Gas permeability measurements are corrected by Klinkenberg

effect and the absolute permeability values are shown in **Table 3**.

Table 3: Absolute permeability of fractured core

Overburden pressure, bar	*Absolute permeability mD*
27	1.63
57	0.89
97	0.56
145	0.45

By comparing liquid and absolute permeability measurements on fractured core, it's clear that the absolute permeability is five to six times higher than liquid permeability. This significant difference is most likely due to the following:

- Incompatibility between injecting brine and in place brine results in clay swelling and core plugging.
- Fine migration due to high pressure water injection.

The nature of initial water in place is not recognized yet. Therefore, to reduce the effect of clay swelling, after each pressure increment, the core is removed from core holder and washed by methanol and then dried.

Figure 4 is showing the comparison of permeability reduction by injecting brine and nitrogen into the fractured core at the same operating conditions.

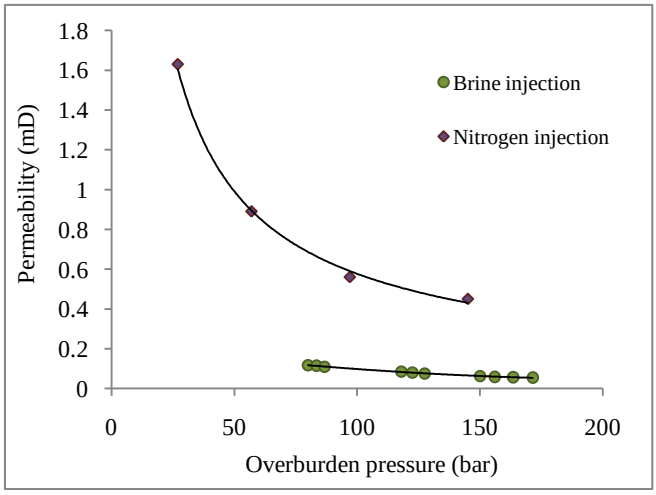

Figure 4: Permeability measured by brine and nitrogen

Since the cores are plugged from sequential depth, lithologies of both cores are almost the same. For this reason, the unfractured core is representative of the matrix properties in fractured core. The centrifuge method was used to measure the capillary pressure of fully water saturated core. **Figure 5** shows the drainage capillary pressure curve versus average water saturation for unfractured core.

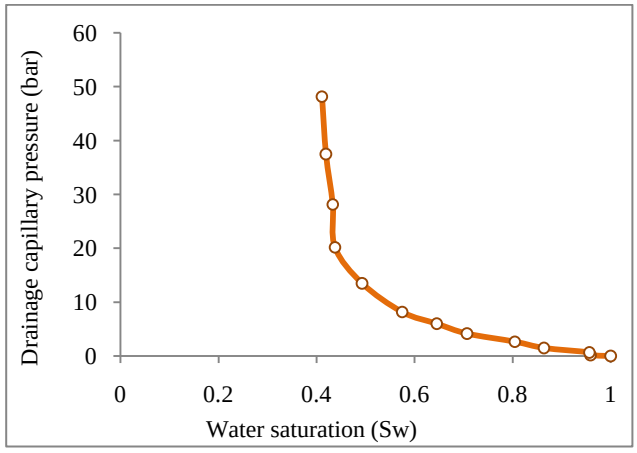

Figure 5: Drainage capillary pressure for air-water system

Since the core is very tight, an unsteady state drainage relative permeability test is performed with following procedure:

1. Spinning the core at a certain speed in the centrifuge and recording appropriate water saturation
2. Passing air through the core at that water saturation at constant pressure gradient (20 bar)
3. Calculating air effective and relative permeability

Figure 6 shows drainage gas relative permeability curve which is measured by the procedure presented here.

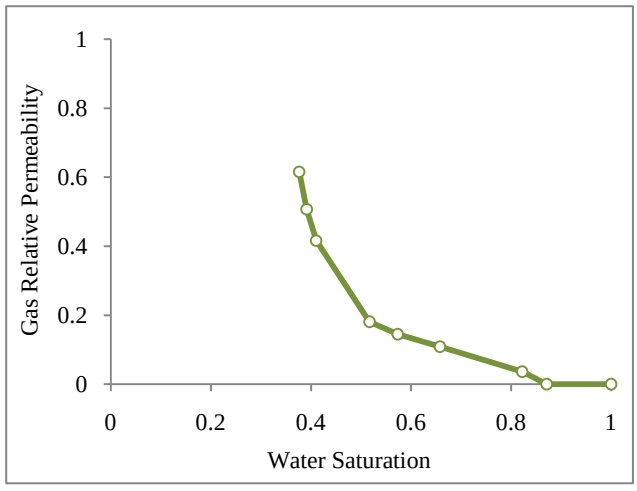

Figure 6: Drainage air relative permeability curve

Experimental data Analysis

In order to properly quantify the effect of fracture permeability on the fluid flow, it is important to understand

the equations describing the changes of this parameter under different overburden pressures. The permeability of a single fracture with laminar flow can be derived from Poiseuille's law:

$$k_f = w^2/12 \quad (1)$$

Where w is fracture width. By the concept of parallel flow, the equation for total flow rate (or injection rate) is:

$$Q_t = Q_f + Q_m \quad (2)$$

Where Q_t, total flow rate, Q_f, fracture flow rate and Q_m is matrix flow rate.

Since the flow rates were measured at steady state conditions, the pressure drop in the matrix and fracture would be the same. Thus, the above equation can be simplified to:

$$k_f = \frac{k_{av}A - k_m(A - wl)}{wl} \quad (3)$$

Where k_{av}, k_m and k_f are average, matrix and fracture permeability respectively. A, cross section, w, fracture width and l is core length. Now, we have two equations and two unknowns. So, combining Eqs.1 and 3, we can find the fracture permeability and fracture width. **Table 4** presents the fracture permeability and fracture width under various effective overburden pressure which is obtained by above equations.

Table 4: Fracture permeability and width versus effective overburden pressure

Overburden pressure, bar	*Flow rate ml/min*	*Fracture width,* 10^{-6} *m*	*Fracture permeability, D*
80	0.6	2.27	4.34
83.5	0.5	2.23	4.21
86.75	0.4	2.15	3.91
118	0.4	1.78	2.66
122.5	0.3	1.67	2.35
127.5	0.2	1.53	1.98
159	0.4	1.12	1.06
156	0.3	0.89	0.67
163.5	0.2	0.79	0.53
171.5	0.1	0.69	0.41

As depicted in **Figure 7**, the fracture width is reduced as overburden pressure is increased. Moreover, the flow rate variation, especially at higher overburden pressure, has no significant effect on fracture width.

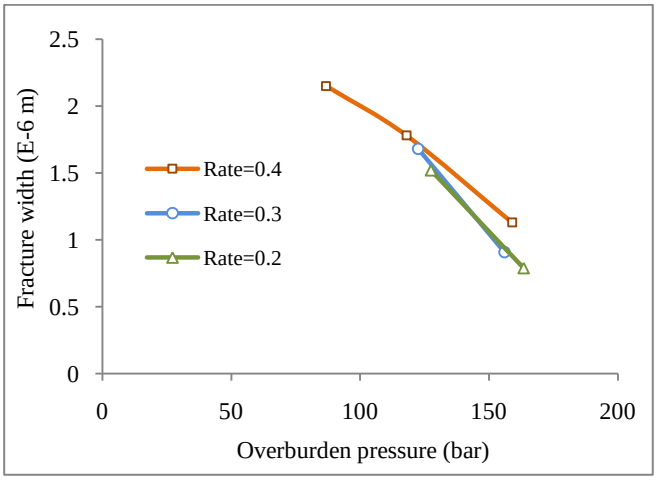

Figure 7: Effect of injection rates on fracture width at various overburden pressures

With reference to Figure 3, we can see that at higher overburden pressure, both fractured and unfractured cores are showing almost the same permeability. It indicates that at the pressures greater than 150 bar, there is no significant difference in fracture and matrix conductivity.

Core scale simulation study

The objective of this section is to use the core scale simulation approach in order to quantify the effect of fracture permeability and aperture variations under different stress conditions on CO_2 storage mechanisms. The simulation tool employed in this study is ECLIPSE 2009 (ECLIPSE, 2009). The laboratory configuration and results, in which the water was injected through the fracture, is matched in this modeling effort. Since the model represents the laboratory core flooding condition very well, it should be appropriate for studying a physical CO_2 injection process.

The simulator can accurately compute the physical properties of pure and impure CO_2 as a function of temperature and pressure (Hurter *et al.*, 2007). With the CO2STORE option, three phases are considered: a CO_2 rich phase, gas phase, an H_2O rich phase, liquid phase and a solid phase. With this option, precise mutual solubilities of CO_2 in water are calculated.

Model geometry and material properties: The rectangular grid block with closed boundary conditions is applied. A three-dimensional domain with 9.6 cm long, 4.25 wide and

4.25 m thick, is capturing complete core bulk volume. The number of fundamental grid blocks is 19×17×22. The grid block size near fracture is reduced to size of fracture aperture to improve accuracy of CO_2 injection behavior. The model geometry is schematically shown in **Figure 8.**

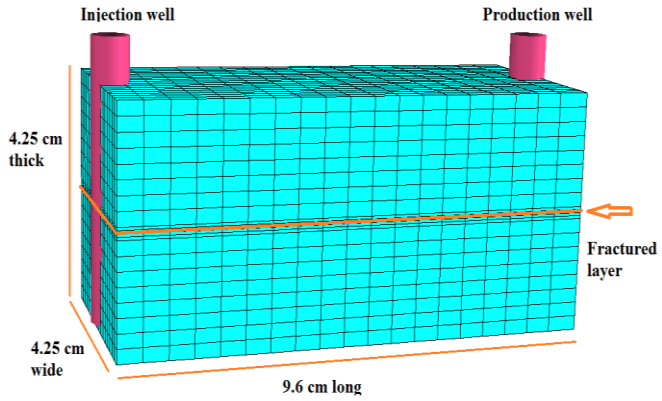

Figure 8: Simulation model geometry

Instead of changing the fracture aperture size at respective overburden pressure, we suppose fixed fracture width, during core flooding. For this purpose, at each overburden pressure, we calculate the equivalent fracture permeability for that fixed fracture width equals 5×10^{-5} m. According to the Darcy equation, if the flow rate is kept constant, the equivalent fracture permeability at each overburden pressure is computed by:

$$k_{fe} = \frac{k_f w}{w_e} = \frac{k_f w}{5 \times 10^{-5}} \quad (4)$$

Where k_{fe} is equivalent fracture permeability.

The well configurations consists of single vertical well injecting water into all layers at one end and a vertical well producing from all layers at opposite the end. Fluid components are CO_2, H_2O, NaCl, although in water injection case, there is no CO_2 component in system. Initial pressure and temperature in model are 28°C and 73 bar respectively. Matrix and fracture porosity and permeability are taken from Tables 1 and 2. Matrix capillary pressure and relative permeability curves are given in Figures 5 and 6 respectively. Zero capillary pressure and straight line relative permeability are applied for the fracture. Horizontal permeability is assumed to be one and a half times higher than in vertical direction as measured previously (Farokhpoor *et al.*, 2010).

Simulation results for water injection tests: To match the experimental results, instead of using different overburden pressures, the respective permeabilities are used in the model. Furthermore, injecting brine with appropriate flow rate, as listed in Table 2, is continued until the steady state pressure is achieved. Simulated mean pressure, as a matching parameter, is compared with observed data. Effective overburden pressure is the difference between confining pressure and mean pressure in the core. Therefore, we can use the effective overburden pressure as a matching parameter instead of the mean pressure. **Figure 9** shows the comparison between laboratory observations and simulation results.

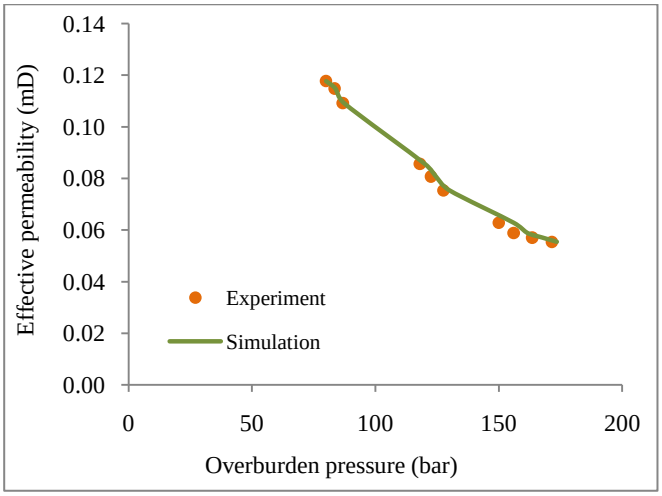

Figure 9: Observed and simulated effective overburden pressure

As shown in Figure 9, the numerical model gives nice match with observed data. Three distinct data points on the graph indicates three confining pressure, 100, 140 and 180 bar. At the lowest confining pressure, 100 bar, the match is perfect. As the confining pressure increases to 140 and 180 bar, simulation predicts lower mean pressure. This prediction can be related to horizontal-vertical permeability ratio. In order to get perfect match, we applied the ratio $k_H/k_V = 1.4$ for 140 bar and $k_H/k_V = 1.3$ for 180 bar). In this case, the quality of the match is excellent. This behavior can be explained by experiment conditions.

During the experiments, different overburden pressures (radial forces) were applied to the cylindrical core, while the axial direction was kept at different pressures. Core is subjected to injection pressure at one end and the opposite end is opened to constant atmospheric pressure. Increasing the confining pressure enlarges radial stress whereas the

axial stress is constant. According to core holder configuration, rising radial stress results in horizontal permeability reduction. Applying fixed ratio for permeability anisotropy does not capture this experimental error in the modeling effort.

Second step is to inject CO_2 into a fully water saturated core in model which is validated by water flooding results. In this case, an injection of CO_2 at a rate of 500 Scm^3/hr for 76 hours is controlled by a maximum bottom-hole pressure (BHP) of 100 bars in order to avoid fracturing. At the opposite end, a production well is placed to produce water and CO_2 and is controlled by a minimum bottom-hole pressure of 60 bar as a back pressure.

Simulation results for CO_2 injection: Since the production well produces at the pressure no higher than 60 bar and CO_2 is injected at low flow rate, simulated mean pressure in the core varies between 60 to 62 bar for all runs. After 76 hours CO_2 injection, around 40 percent of total water in place is produced. At the end of injection the average CO_2 saturation in the core is reached to 40-41 percent for the all permeability range presented here. By increasing permeability, the total volume of gas which is trapped in the core reduces. **Figure 10** presents total amount of CO_2 in place in moles versus effective permeability.

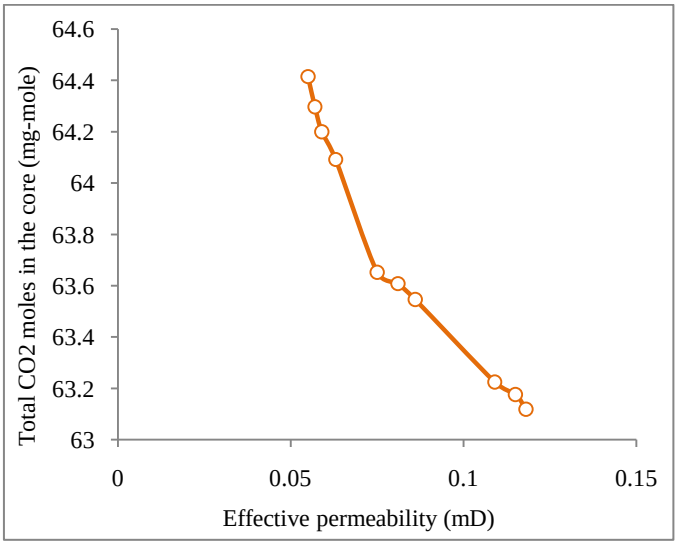

Figure 10: Effect of permeability on total gas in place

As illustrated in Figure 10, as the effective permeability increases, more gas is produced through the high permeable layer. It shows that at higher permeability, the quantity of trapped gas in the core is reduced.

In a CO_2 storage project in a dipping naturally fractured aquifer, where CO_2 rises in an updip direction, it will encounter a fracture with higher permeability. CO_2 breakthrough time is shortened by increased permeability along the bedding plane in updip direction. In **Table 5,** CO_2 breakthrough times at various effective permeabilities are listed.

Table 5: CO_2 breakthrough time versus effective permeability

Effective permeability, mD	*CO_2 breakthrough time, min*
0.118	16
0.115	18
0.109	21
0.086	33
0.081	42
0.075	48
0.063	102
0.059	108
0.057	111
0.055	112

By increasing permeability from k = 0.055 to k = 0.118 mD, CO_2 breakthrough time is reduced from 112 min to 16 min. At lower permeability, CO_2 takes longer time to reach breakthrough as effective permeability decreases. For pressure higher than 150 bar confining pressure, there is no significant difference in breakthrough time. Under these pressures, fracture permeability is reduced to the same level as the matrix permeability. At this situation, increasing overburden pressure has no important effect on CO_2 flow mechanisms. In fractured saline aquifers CO_2 rises up due to buoyancy forces. Moreover, fractures can introduce preferential flow pathways which support and fortify buoyancy effects. Especially when saline formation is tilled in upwards, growing permeability in corporation with buoyancy forces results in higher CO_2 velocity. **Figure 11** shows an element where CO_2 displaces water. CO_2 saturation is shown for the case with k= 0.118 mD at breakthrough time.

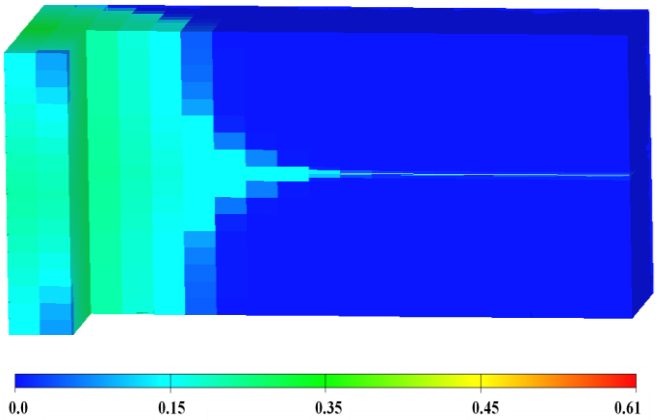

Figure 11: CO_2 saturation in a reservoir element for case with k=0.118 mD at breakthrough time

Although the system is water-wet, and matrix low permeability shows very high capillary pressure (Figure 5), fluid is produced through both fracture and matrix. The fracture contribution in producing fluid changes with overburden pressure and respective permeability. Under higher overburden pressure, less fluid passes through fracture as shown in **Figure 12**.

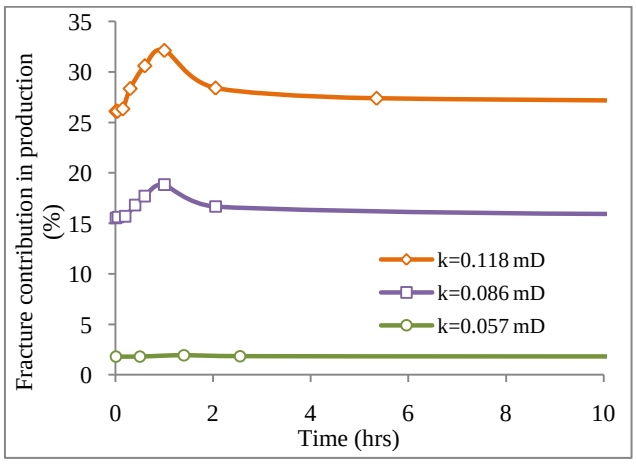

Figure 12: Fracture contribution in producing fluid versus time

In Figure 12, fracture contribution in producing fluid reduces significantly by decreasing permeability. At constant permeability, the amount of fluid produced through the fracture is constant during the injection except at CO_2 breakthrough time. Under high overburden pressure (170 bar), fracture conducts only 2 percent of total produced fluid. Whereas, in case of k = 0.118 mD, the fracture produces 27 percent of total fluid production. **Figure 13** compares CO_2 saturation for these three cases at 36 minutes after injection started.

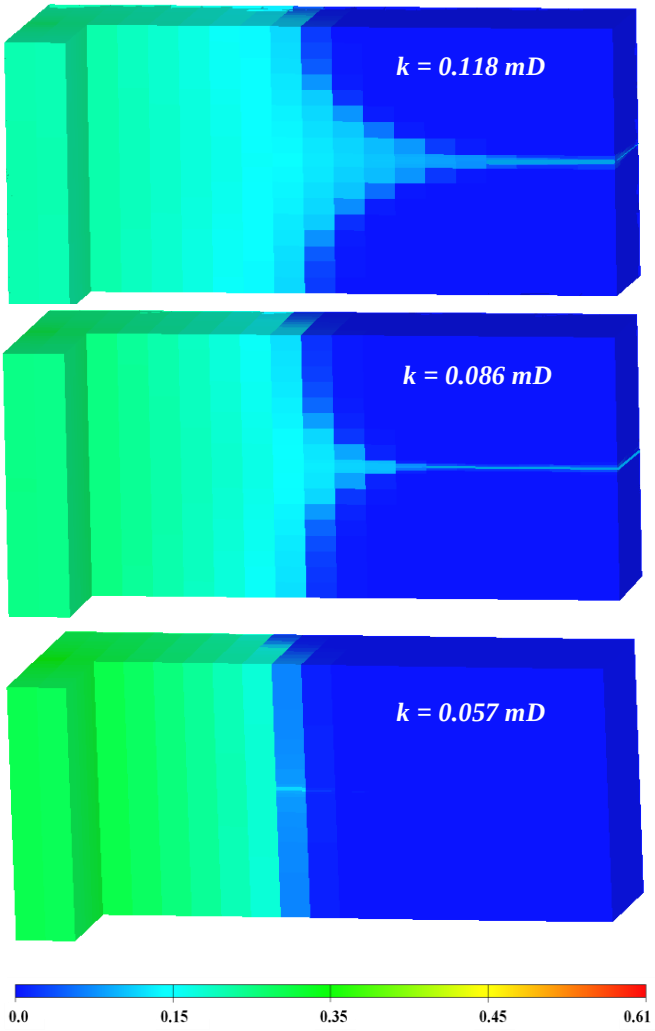

Figure 13: CO_2 saturation for three different permeabilities

One of the main storage mechanisms for CO_2 that operates in reservoir rock is dissolution trapping in which injected CO_2 dissolves in brine and will be trapped. The employed simulator option has the ability to calculate precise mutual solubilities of CO_2 in water for fine grid blocks. The amount of CO_2 mobile gas phase and dissolved CO_2 in brine inside the core at the end of injection period is gathered in **Table 6**. As reported in Table 6, by increasing the core permeability, the quantity of CO_2 as mobile gas phase and as dissolved phase in brine decreases. On the other hand, at higher permeabilities, as illustrated in Figure 10, the total amount of CO_2 moles in place reduces. While CO_2 phase trapping is reduced, the amount of dissolution trapping will have a proportionate reduction. According to Table 6, increasing overburden pressure from 100 to 180 bar, will increase the quantity of CO_2 free phase and CO_2 dissolution in brine by 2.5% and 0.5 % respectively.

Table 6: Amount of free CO_2 and dissolved CO_2 in brine at the end of injection at various permeabilities

Permeability, mD	*CO_2 dissolved mg-M*	*CO_2 mobile phase, mg-M*	*Mean pressure, bar*
0.118	16.28	46.83	60.54
0.115	16.28	46.90	60.55
0.109	16.28	46.94	60.58
0.086	16.30	47.32	60.74
0.081	16.30	47.40	60.78
0.075	16.31	47.25	60.84
0.063	16.34	47.76	61.00
0.059	16.35	47.85	61.07
0.057	16.35	47.94	61.11
0.055	16.35	48.06	61.16

As reported in Table 6, after 76 hours CO_2 injection, 75 percent of total CO_2 in the core is presented as a free phase and 25 percent is dissolved in the brine. As the permeability decreases from k = 0.118 to k = 0.055 mD, the quantity of CO_2 as a free gas is increased by 2.6 percent. The amount of CO_2 dissolution in brine phase is increased by decreased permeability but it is not significant. The CO_2 solubility in brine phase is strongly affected by mean pressure. At the end of injection, the mean pressure for all cases is almost the same and it changes around 1 bar from highest permeability to lowest permeability. Consequently, the reported values for CO_2 dissolution in brine phase are affected mainly by permeability and total gas in place.

Conclusion

1. Experimental data shows that increasing overburden pressure resulted in effective permeability reduction. From 10 to 180 bar overburden pressure, permeability in fractured core and unfractured core is reduced by 73 and 24 percent respectively.

2. In a dipping naturally fractured aquifer and in updip direction, permeability increases with decreasing overburden pressure. If CO_2 is injected in deep parts of the reservoir, it rises up due to buoyancy forces in pathways with high permeabilities. This phenomenon is important in assessing the capacity for secure storage in an aquifer.

3. Numerical simulation results show that fractures bring preferential pathways for CO_2 flow. Through the fractures CO_2 moves faster with larger buoyancy forces and lower capillary pressure. Compare to unfractured system, it leaves less time for CO_2 to be trapped as residual phase.

4. Fracture contribution in producing fluid is reduced from 27 to 2% of total production when overburden pressure is increased from 100 to 180 bar. Simulation results show that production occurred from both matrix and fracture from start to end of production.

5. While CO_2 phase trapping is reduced, the amount of dissolution trapping is diminished proportionally. In our simulation, under increasing overburden pressure from 100 to 180 bar, the quantity of CO_2 as free gas and as dissolved phase in brine is increased by 2.5% and 0.5% respectively.

Acknowledgments

The authors gratefully acknowledge the support from the $BIGCO_2$ project. This publication is number 2 from "The Longyearbyen CO_2-Lab".

Nomenclature

A	=Cross section (m^2)
k_f	=Fracture permeability (m^2)
k_{av}	=Average permeability (m^2)
k_m	=Matrix permeability (m^2)
k_{fe}	=Equivalent fracture permeability (m^2)
k_H	=Horizontal permeability (m^2)
k_V	=Vertical permeability (m^2)
l	=Core length (m)
Q_t	=Total flow rate (m^3/hr)
Q_f	=Fracture flow rate (m^3/hr)
Q_m	=Matrix flow rate (m^3/hr)
w	=Fracture width (m)
w_e	=Equivalent fracture width (m)

Reference

ECLIPSE. (2009). Technical Description.

Farokhpoor, R., Torsæter, O., Baghbanbashi, T., Mørk, A., & Lindeberg, E. (2010). Experimental and Numerical Simulation of CO2 Injection into Upper-Triassik Sandstones in Svalbard, Norway. *Paper SPE 139524 presented at the SPE International CO2 Conference.* New Orleans: SPE 139524-MS.

Huo, D., & Gong, B. (2010). Discrete Modeling and Simulation on Potential Leakage through Fractures in CO2 Sequestration. *Paper*

SPE 135507 presented at the SPE Annual Technical Conference and Exhibition. Florence: SPE 135507-MS.

Hurter, S., Labregere, D., & Berge, J. (2007). Simulations for CO2 Injection Projects With Compositional Simulator. *Paper SPE 108540 presented at the Offshore Europe.* Aberdeen: SPE 108540-MS.

Mørk, M., & Farokhpoor, R. (2011). Petrogrephy of Low Permeability Triassic—Jurassic Sandstones from the Longyearbyen Drill-Holes DH4 and DH2. *Abstract presented at Winter Conference, NGF Abstracts and Proceedings of the Geological Society of Norway*, (pp. Number 1, 67-68. ISBN 978-82-92394-62-5). Stavanger.

Olaussen, S., Braathen, A., Hansen, T., Johansen, T., Mørk, A., Mørk, M., et al. (2011). Results from Characterization and Testing of a Low-Pressured Unconventional Reservoir, the Triassic De Geerdalen Formation in well DH4 Longyearbyen CO2 lab, Adventdalen, Svalbard. *Abstract presented at Winter conference, NGF Abstracts and Proceedings of the Geological Society of Norway*, (pp. Number 1,73-74. ISBN 978-82-92394-62-5). Stavanger.

Senger, K., Ogata, K., Tveranger, J., & Braathen, A. (2011). Towards Simulation of CO2 Flow Through a Naturally Fractured Reservoir, Spitsbergen, Svalbard. *Poster presented at NARG Fractured Reservoirs Workshop.* Manchester: http://www.cipr.uni.no/person.aspx?person=1070.